Design of a GaAs-based guided-wave heterodyne circuit for signal processing

Mario N. Armenise, Vittorio M.N. Passaro

Politecnico di Bari
Dipartimento di Elettrotecnica ed Elettronica
Via E. Orabona 4
70125 Bari, Italy
Tel. +39-80-242492, FAX N.+39-80-242315
E-mail: BITNET at ARMENISE%IBADEE.BA.INFN.IT
@ VM.CNUCE.CNR.IT

Abstract

In this paper, we present the design of a GaAs-based heterodyne guided-wave circuit for signal processing. The circuit includes two acoustooptic Bragg cells, a grating concave lens and a grating focusing lens for performing heterodyning mode interference. Significant improvements in terms of single and double tone dynamic range have been obtained with respect to homodyne architectures.

Introduction

In the last few years, the optoelectronics technologies are becoming more and more mature for fabricating a number of active and passive guided-wave devices, to be used in complex circuits for signal processing, optical computing and sensing applications [1-2]. The interest devoted to the optical architectures is mainly due to the advantages allowed with respect to analogous electronic devices and circuits, in terms of lower power consumption, higher data throughput, smaller size and weight, larger bandwidth, and lower sensitivity to environmental parameters.

One of the fundamental elements of a number of guided-wave processors is the spatial light modulator, in which the collimated laser beam can be modulated by a set of external signals by exploiting the acousto-optic (AO), electro-optic, photo-refractive or magneto-optic effect. Spatial modulators based on the guided-wave acousto-optic Bragg cell [3] show some interesting characteristics for signal processing operations, such as high linear dynamic range and high diffraction efficiency.

Many guided-wave circuits based on AO Bragg cells have been already proposed and demonstrated for performing spectral analysis, convolution, correlation, and multichannel radar applications [4]. As for the spectral analysis, which we are dealing with in this paper, some homodyne optical circuits have been proposed showing significant advantages with respect to discrete devices, together with an intrinsic low dynamic range [1] (< 25 dB), due to the squared response of output photodiode array. In this work, improvements of dynamic range have been achieved by using a heterodyne detection configuration. In the following sections, a detailed description of the design parameters of the circuit is given.

Processor architecture

The schematic diagram of the circuit we propose is reported in Fig.1, in which optical heterodyning is performed by interfering the diffracted beam coming out from the AO Bragg cells with a reference beam, to detect at the output just the signal amplitude to be processed and so to improve the dynamic range. The spectrum analyzer we have designed includes a guiding $Al_{0.1}Ga_{0.9}As$ /$Al_{0.25}Ga_{0.75}As$ / GaAs double heterostructure. The guided beam is expanded and collimated by a double integrated grating having non linear groove profile. The AO cells consist of a pair of uniform electrode interdigital transducers, working at the center radiofrequency of 230 and 345 MHz, respectively. A concave grating lens produces the reference beam from the undiffracted AO beam, and a final integrated lens focuses both the beams (the diffracted beam and the reference one) on the output photodiode array.

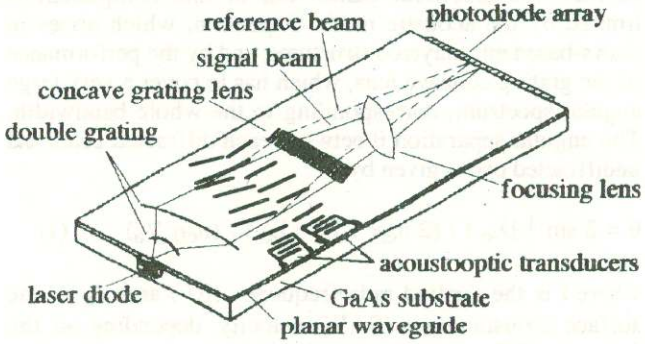

Fig.1. Architecture of the GaAs heterodyne circuit.

Processor design

All the design parameters have been calculated for each integrated component of the circuit at the free-space optical wavelength of 0.85 μm.

A. Waveguide

The optical waveguide is formed by an AlGaAs/AlGaAs/GaAs double heterostructure. We have designed an $Al_{0.1}Ga_{0.9}As$ guiding layer (thickness 0.8 μm, refractive index 3.587) over an $Al_{0.25}Ga_{0.75}As$ buffer layer, 3 μm thick with refractive index 3.521, laying on the GaAs substrate, having refractive index 3.63. This structure supports the fundamental mode of both the polarizations with very similar effective indices, namely n_{eff} =3.564 (TE_0) and n_{eff} =3.562 (TM_0). This characteristic allows to have the same diffraction behaviour of both the polarizations, thus improving the grating efficiencies.
Moreover, because of the poor piezoelectric effect occurring in the GaAs material and related compounds, an additional ZnO layer has been considered in the AO interaction regions, which enables the efficient operation of the SAW transducers. We denote with I the waveguide region without ZnO layer and with II the region with it. A ZnO layer thickness of 0.2 μm has been evaluated in order to

minimize the influence of the ZnO layer on the optical mode confinements. The design parameters of planar waveguide are given in Table I.

Table I: Planar waveguide parameters.

Optical wavelength		$\lambda_o = 0.85\ \mu m$
Effective index - region I	(TE_o)	$n_{eff} = 3.564$
	(TM_o)	$n_{eff} = 3.562$
Effective index - region II	(TE_o)	$n_{eff} = 3.565$
	(TM_o)	$n_{eff} = 3.563$

B. Acoustooptic Bragg cells

The central point of the design of both the AO Bragg cells is the choice of the centre frequency f_c and the bandwidth. In fact, the electrical bandwidth of this component is limited by the acoustic mode dispersion, which arises in GaAs-based multilayered structures, and by the performance of the grating concave lens, which has to cover a very large angular spectrum, corresponding to the whole bandwidth. The angular separation θ between each diffracted beam and undiffracted one is given by:

$$\theta = 2 \sin^{-1} [\lambda_o f / (2 n_{eff} V_a)] \approx \lambda_o f / (n_{eff} V_a) \qquad (1)$$

where f is the applied radiofrequency (RF) and V_a is the surface acoustic wave (SAW) velocity, depending on the frequency f. By derivating Eq.(1), we have:

$$d\theta/df = \lambda_o [1 - f/V_a\, dV_a/df]\, df/(n_{eff} V_a) \qquad (2)$$

Also, the velocity dispersion affects the minimum distance between two adjacent photodetectors Δy:

$$\Delta y = F \Delta\theta = \lambda_o \Delta f [1 - f/V_a\, dV_a/df] /(n_{eff} V_a) \qquad (3)$$

where F is the focal length of output focusing lens and Δf the frequency resolution of the device. If we assume that V_a= cost, the percentage change of θ is given by:

$$(\theta - \theta_o)/\theta = (1/V_a - 1/V_o)/1/V_a = \varepsilon \qquad (4)$$

where θ_o and V_o are reffered to the same frequency f_o, and V_a is the approximated value and V_o the exact value of SAW velocity.
Therefore, the maximum error on θ is equal to the error on V_a, namely ε. In the design, we have assumed a transducer bandwidth B =180 MHz and a centre frequency f_c =270 MHz. The maximum frequency for each transducer to be used is then f_1 =180 MHz and f_2 =360 MHz. The bandwidth has been limited to an octave in order to avoid the spurious signals, generated by the intermodulation products in the AO regions. The acoustic velocities have been calculated by using a complete model [3], and are given by:

$$f = 180 \text{ MHz} \Rightarrow V_a = 2784 \text{ m/s}$$
$$f = 270 \text{ MHz} \Rightarrow V_a = 2804 \text{ m/s} \qquad (5)$$
$$f = 360 \text{ MHz} \Rightarrow V_a = 2813 \text{ m/s}$$

whose change being less than 1.1% over the whole bandwidth. In order to design an acoustic cell having the large bandwidth B=180 MHz, a number of different configurations of interdigital transducers can be considered: a single periodic interdigital, a single aperiodical interdigital with tilted electrodes or a multiple tilted periodic electrode geometry. The third solution has been preferred, because of its easier fabrication procedure, of the lower power consumption and of less sensitivity to dimensional errors allowed with respect to the other two.
The fractional bandwidth of the whole component can be expressed by:

$$\Delta B/f_c \approx 1.8\, n_{eff} V_a \cos(\theta_B)\, \Lambda /(\lambda_o f_c L) \qquad (6)$$

where θ_B and Λ represent the Bragg angle and the SAW wavelength at the centre frequency f_c. L is the transducer aperture. By a computer-aided design procedure, we have found the optimized number of transducers equal to two. The values of all the transducer parameters are summarized in Table II. The cut of the GaAs substrate was (100) and the SAW propagation direction was (010) which, from data reported in literature [5], represent the best orientations in terms of diffraction efficiency, dynamic range, frequency resolution and SAW isotropic behaviour.

Table II. SAW transducer parameters.

Transducer number		2
Centre radio frequencies	(1)	230 MHz
	(2)	345 MHz
Transducer length	(1)	3.0 mm
	(2)	2.2 mm
Power consumption	(1)	1.8 mW
	(2)	3.0 mW
Tilting angle		0.56°
		0.85°
Electrical bandwidth	(1)	118 MHz
	(2)	135 MHz
3-dB Bragg bandwidth	(1)	90 MHz
	(2)	81 MHz
Quality factor	(1)	17.5
	(2)	36.5
Electrode number	(1)	4
	(2)	5
Electromechanic coupling coefficient		0.024
Electrode static capacitance		0.3 pF
		0.2 pF
Transdution efficiency	(1)	- 11.9 dB
	(2)	- 9.1 dB

Fig.2 shows the geometry of both the AO cells.
The diffraction efficiency of the pair can be written as:

$$\eta_T = \eta_1 (1- \eta_2) + \eta_2 (1- \eta_1) + 2H \sqrt{[\eta_1 (1-\eta_1) \eta_2]} \qquad (7)$$

where η_1 and η_2 are the diffraction efficiencies of the single AO cells. The numerical parameter H depends on the applied RFs and has a significant value at intermediate frequencies. Moreover, it strongly depends on the phase shifts between the SAWs, i.e. $\Delta\Phi_{12} = \Phi_2 - \Phi_1$ and assumes a high value over the whole transducer bandwidth when $\Delta\Phi_{12}$=250°. The separation between the two cells can be expressed by:

$$\Delta x_{12} = D_s - L_1/2 - L_2/2 \cos(\Delta\theta_B) = 0.59 \text{ mm} \qquad (8)$$

where

$$D_s = 2 M \Lambda_i 2/\lambda_o \qquad (9)$$

and Λ_i is the SAW wavelength at intermediate frequency $f_c=(f_1+f_2)/2$. Fig.3 illustrates the diffraction efficiency η_T as a function of applied frequency when $\Delta\Phi_{12}$=250° by using an appropriate phase shift network.

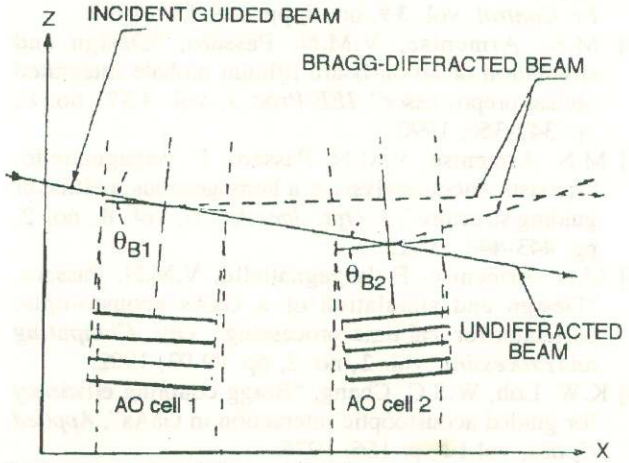

Fig.2. Geometry of the two AO Bragg cells.

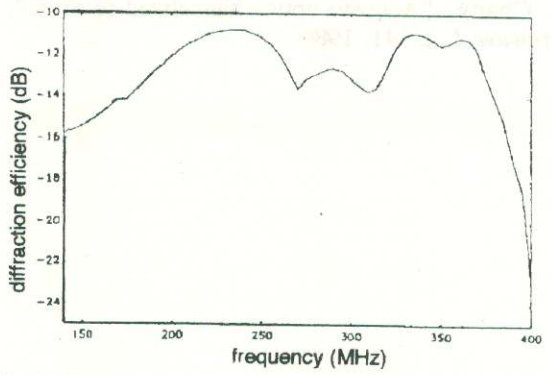

Fig.3. Transducer diffraction efficiency over the bandwidth, at $\Delta\Phi_{12}$=250°.

C. Grating concave lens

The concave lens has to diffract the undiffracted and collimated beam coming from the AO Bragg cells, in order to cover the whole angular range of all the diffracted beams. The concave lens allows to obtain a heterodyne detection at any beam direction over the whole bandwidth. Obviously, a correct operation of the lens would require the reduction as much as possible of the losses due to unwanted deflection, to have the maximum signal-to-noise ratio at the output and to assure uniform diffraction behaviour for each signal beam propagating along different directions. Since the angular bandwidth ranges from 0.88° to 1.76°, corresponding to the bandwith 180-360 MHz, the focal length f_l and the intersections points of the lens with the focal line are:

$$\begin{aligned} f_l &= D/(\tan(\theta_2) - \tan(\theta_1)) = 16.32 \text{ mm} \\ x_1 &= f_l \tan(\theta_1) = 2.5 \text{ mm} \\ x_2 &= f_l \tan(\theta_2) = 5 \text{ mm} \end{aligned} \qquad (10)$$

where D=2.5 mm is the optical beam aperture. The other design parameters have been calculated in order to have a 100% diffraction efficiency over the whole angular bandwidth: in such a way, the groove number, period, width and depth have been determined, as it is shown in Table III.

Table III. Design parameters of concave lens.

Lens aperture	2.5 mm
Lens thickness	0.29 mm
Focal length	16.5 cm
Groove number	242
Groove tilting angle	1.31° - 1.75°
Groove period	7.8 - 15.7 μm
Groove width	1.9 - 3.9 μm
Groove depth	26 nm

The lens diffraction efficiency as a function of the angle of incidence has been calculated. The results obtained assert that, for an average (11.5 μm) value of the grating period, a small reduction (0.5 dB) of the diffraction efficiency is found in the variation range of incident angles -0.4 : +0.4°.

D. Grating focusing lens

The focusing lens has to focuse the mode diffracted by the concave lens on the photodetector array. The design parameters are summarized in Table IV and have been calculated in order to maximize the diffraction efficiency of the lens over the whole angular bandwidth. The parameters utilized are analogous to those of the grating concave lens.

Processor performance

The performance of our heterodyne architecture have been calculated in terms of wavelength dispersion and dynamic range. If we consider a change $\Delta\lambda_o$ of the free-space optical wavelength, emitted by a laser diode and coupled into the planar waveguide, the corresponding variation of the diffraction angle of the generic beam can be written as:

$$\Delta\theta = f_c \, \Delta\lambda_o / (n_{eff} \, V_a) \qquad (11)$$

Since the frequency resolution Δf depends on the relationship:

$$\Delta f = n_{eff} \, V_a \, \Delta\theta / \lambda_o \qquad (12)$$

it is clear that, being Δf =1.8 MHz, the maximum change of λ_o can be $\Delta\lambda_o$ =56.7 Å. Distributed feedback laser diode or distributed Bragg reflector can easily satisfy this requirement.

Moreover, the size S of active area of each photodetector must be large enough to appropriately detect the beam at its own proper angle. The expression to be satisfied is:

$$S \geq 1.64 \, \lambda_o \, F/(n_{eff} \, D) \approx 3 \, \mu m \qquad (13)$$

The number of different channels of the circuit, corresponding to different photodiodes of the array, is given by N =B/Δf = 180 /1.8 =100.

To evaluate the single-tone dynamic range DR_h [6], the following equation can be considered:

$$DR_h = 2 \, DR - 10\log[B/(25 \, \Delta f)] + 10\log(1 - \eta_g) \qquad (14)$$

where DR is the dynamic range of an equivalent homodyne circuit and η_g is the diffraction efficiency of grating concave lens. By assuming an optical propagation loss α=1 dB/cm, a laser diode power of 10 mW, a collimating grating efficiency of -3 dB, and a NEP factor of each photodiode of -50dB, we obtain DR =33 dB. In our circuit, Eq.(14) gives a much higher value of dynamic range, DR_h =57 dB, being η_g =0.5.

The double-tone dynamic range, which depends on the influence of the intermodulation products in the heterodyning mixing process, has been also calculated [6] as:

$$DR_h = 4/3 \, \{+50 + 10\log\sqrt{[A \, \eta_g(1 - \eta_g) / N]} \} - 10 = 48.5 \text{ dB} \qquad (15)$$

where A is a constant. This value represents a significant improvement with respect to the analogous quantity in the homodyne detection, i.e. DR =28.7 dB.

Table IV. Design parameters of focusing lens.

Lens aperture		D = 2.5 mm
Lens thickness		0.29 mm
Focal length		f_1 = 20 mm
Number F =f/D		F = 8
Q factor		15
Lens coordinates	(1)	x_1 = 1.2 mm
	(2)	x_2 = 1.3 mm
Groove number		N = 328
Groove tilting angle		-0.55° - 3.02°
Groove period		4:342:3.7 μm
Groove width		1:85:0.92 μm
Groove depth		33 nm
Focusing efficiency		89 %

Conclusions

The design of a novel GaAs-based guided-wave circuit for heterodyning detection of RF signals has been presented. The architecture we propose allows to improve the linear and double-tone dynamic range with respect to other homodyne guided-wave configurations, having similar performance in terms of frequency resolution, bandwidth and requirement of optical wavelength dispersion. In this circuit the number of channels has been assumed equal to 100, the electrical bandwidth is 180 MHz around the center frequency of 270 MHz and the channel frequency resolution is 1.8 MHz. The calculated single- and double-tone dynamic range are 57 dB and 48.5 dB.

References

[1] C.S. Tsai, "Integrated Acoustooptic Circuits and Applications", *IEEE Trans. Ultrason., Ferroelec. and Fr. Control*, vol. **39**, no. 5, pp. 529-554, 1992.

[2] M.N. Armenise, V.M.N. Passaro, "Design and simulation of an on-board lithium niobate integrated optical preprocessor", *IEE Proc. J*, vol. **137**, no. 6, pp. 347-356, 1990.

[3] M.N. Armenise, V.M.N. Passaro, F. Impagnatiello, "Acoustic-mode analysis of a homogeneous multilayer guiding structure", *J. Opt. Soc. Am. B*, vol. **8**, no. 2, pp. 443-448, 1991.

[4] M.N. Armenise, F. Impagnatiello, V.M.N. Passaro, "Design and simulation of a GaAs acousto-optic correlator for real time processing", *Opt. Computing and Processing*, vol. **2**, no. 2, pp. 79-93, 1992.

[5] K.W. Loh, W.S.C. Chang, "Bragg coupling efficiency for guided acoustooptic interaction in GaAs", *Applied Optics*, vol.**15**, p. 156, 1976.

[6] A; Vanderlugt, "Interferometric spectrum analyzer", *Applied Optics*, vol.20, p.2770, 1981.

[7] I.C. Chang, "Acousto-optic channelized receiver", *Microwave J.*, p.141, 1986.